Scientific Research Publishing

Open Journal of Applied Sciences, 2025, 15(11), 3648-3662
https://www.scirp.org/journal/ojapps
ISSN Online: 2165-3925
ISSN Print: 2165-3917

Analysis of Falkner-Skan Equation of an Unsteady Dusty Fluid Flow over a Horizontal Wedge

Mohammad Rafiqul Islam*, Abdullah Abu Syed, Md. Alamin Sheikh, Muntasir Ahmed Tanmoy, Tithi Rani Mallick, Jyonto Sarkar

Department of Mathematics, Gopalganj Science and Technology University, Gopalganj, Bangladesh
Email: *mribsmrstu@yahoo.com

How to cite this paper: Islam, M.R., Syed, A.A., Sheikh, M.A., Tanmoy, M.A., Mallick, T.R. and Sarkar, J. (2025) Analysis of Falkner-Skan Equation of an Unsteady Dusty Fluid Flow over a Horizontal Wedge. *Open Journal of Applied Sciences*, **15**, 3648-3662.
https://doi.org/10.4236/ojapps.2025.1511237

Received: October 16, 2025
Accepted: November 18, 2025
Published: November 21, 2025

Abstract

This study aims to analyze the application of boundary layer theory to the Falkner-Skan equation for unsteady laminar boundary-layer flow over a horizontal wedge. The analysis is motivated by the importance of understanding the flow behavior characteristics of unsteady fluids over a horizontal wedge. The governing partial differential equations, along with the relevant boundary conditions, are solved numerically. The constant coefficients in the estimated solution are obtained using the finite difference approximation combined with a trial-and-error approach. Computational results are presented graphically for various values of the non-dimensional parameters involved in the analysis. The study investigates the effects of the fluid concentration parameter, Reynolds number, wedge angle parameter, and particle mass parameter. It is expected that the present findings will contribute to a deeper mathematical understanding of unsteady dusty fluid flow over a horizontal wedge and stimulate further research in this field.

Keywords

Dusty Fluid, Horizontal Wedge, Unsteady Flow, Finite Difference Method, Falkner-Skan Equation

1. Introduction

The steady two-dimensional laminar boundary layer that develops on a wedge or in flows where the surface is not aligned with the flow direction is described by the Falkner-Skan boundary layer, named after Falkner and Skan. It also serves as a classic example of flow over a flat plate subjected to a pressure gradient along its

length, a situation commonly encountered in wind tunnel experiments. The Falkner-Skan [1] extends the Blasius boundary layer model, which applies to flat plates with no pressure gradient, by incorporating pressure gradient effects.

For the boundary layer flow of a homogeneous incompressible fluid of second grade past a wedge positioned symmetrically with respect to the flow direction, non-similar solutions are developed. It is addressed how the skin friction varies in relation to non-Newtonian factors. Rajagopal *et al.* [2]. The angle of the wedge is taken as $a\pi$. Due to the case of unsteady flow, the velocity potential of uniform flow is considered as $U(x,t)$. In the case of flow over a wedge, the velocity potential is assumed to be proportional to a power of distance along the wall. In this analysis, a constant $\tilde{C}$ is introduced that depends on the boundary layer thickness, and it has been treated as a dimensionless measure of the unsteadiness parameter. Regarding the two-dimensional flow, the coordinate system is considered as two-dimensional. Because of the no-slip boundary condition, the results of this solution demonstrate lower skin friction or shear stress, boundary-layer thickness, velocity thickness, and momentum thickness.

Non-Newtonian fluids can transport mass, heat, and momentum; they have grown in significance in industrial and engineering applications. Non-Newtonian fluids are defined as liquids without Newtonian viscosity. There are technical and industrial uses for non-Newtonian fluids. There are some liquids in nature without Newtonian viscosities. Applesauce, polymer mixes, colloidal and fermented mixtures, mud, edibles, paper paste, slush, paints, lubricants, clay glazes, slush, shampoos, and so on are examples of these fluids. It is impossible to forecast the rheological characteristics of non-Newtonian liquids using just shear and stress rates. As a result, the three main types of non-Newtonian liquids are differential, integral, and rate. Numerous investigations of differential fluid flows in various geometries have been conducted. Shear thinning, shear thickening, and a normal stress are characteristics of these liquids; however, the effects of relaxation and retardation durations are not well represented by the differential fluid flow model.

Because this topic has several applications in engineering processes, there has been a significant surge in the last few decades in the research of nano fluid flow across an elongating sheet. A fundamental process with a plethora of applications is heat transfer. The rate of heat transfer, which is used to calculate the amount of heat required by machinery and processes, is dependent on thermal conduction in running liquids. Liquids with nanoparticles added to them significantly enhance the properties of the basic fluids, resulting in nano-fluids. The unsteady flow and heat transfer of a dusty fluid have a wide range of applications in air conditioning, refrigeration, chemical processing, pumps, and nuclear reactors. Datta *et al.* [3] obtained the solution of unsteady heat transfer to pulsatile flow of a dusty viscous incompressible fluid in a channel. In a boundary-layer study, the coupled convection along a vertical non-isothermal wedge buried in a porous material that was saturated with fluid was studied by Kumari & Gorla [4]. In their study, Hossain *et al.* [5] investigated the forced flow of a viscous incompressible

fluid in two dimensions via a horizontal wedge with consistent flow of surface heat, and also represented that the laminar two-dimensional unsteady mixed-convection boundary-layer flow of a viscous incompressible fluid past a sharp wedge has been studied by Hossain *et al.* [6]. Attia [7] investigated an unsteady MHD Coutte flow and heat transfer of dusty fluid. Rajput *et al.* [8] discussed the unsteady nonlinear mixed convective flow of nanofluid over a wedge. Watanabe [9] analyzed the behavior of heat transfer under forced environments where the convection flow is stimulated by a wedge towards suction and injection. This was later studied by Ishak *et al.* [10], who evaluated the two-dimensional boundary layer flow of viscous fluid induced by a moving wedge. Mahanthesh *et al.* [11] investigated the influence of nonlinear convective transport on non-Newtonian Dusty fluid flow through a stretched sheet. The impact of thermal radiation of squeezed dusty fluid flow with heat transfer between parallel plates was studied by Abbas [12]. Chandrawat *et al.* [13] studied numerically the unsteady flow of two immiscible micropolar and dusty fluids through a horizontal plate. In all these investigations, the paper's goal is to investigate an unstable laminar flow of an incompressible conducting viscous dusty fluid between two parallel plates that are endlessly non-conducting, with the porous medium enclosing the upper plate by Parul Szxena *et al.* [14]. Islam *et al.* [15] discussed about on the unsteady laminar flow of heat transferable dusty fluid between two parallel Riga plates. Attia *et al.* [16] prescribed the finite difference approach to solve the coupled unsteady power-law conducting fluid flow and the continuous dusty viscous fluid flow under the influence of a magnetic field. Last few years, some of the authors [17]-[19] have analyzed the phenomenon of dust particles of Newtonian and non-Newtonian fluids with or without heat transfer between parallel plates.

From the above discussion, it follows that no author has previously given any clear idea about the unsteady dusty fluid flow over a horizontal wedge. Our main investigation is the unsteady dusty fluid flow over a horizontal wedge. The behavior of the flow properties is discussed and presented graphically. Here we want to focus on the study on Numerical Study on the Dusty Fluid along the horizontal System, which is also a significant use in the various practical field. The flow characteristics behavior has been illustrated visually, and a brief discussion of their important applications in several real-world fields follows.

2. Mathematical Formation

Consider an unsteady, viscous incompressible dusty fluid that flows along a semi-infinite horizontal wedge at $y=0$ moving with a constant velocity $U(x,t)$. Suppose the direction of flow be taken along the *x*-axis. In the case of flow over a horizontal wedge, the velocity potential is assumed to be proportional to a power of distance along the wall. Under this consideration, the potential flow velocity of the wedge can be written as

$$U(x,t)=\frac{\upsilon x^m}{\delta^{m+1}},$$

where m is a constant, δ is the time-dependent length scale, which is taken to be $\delta = \delta(t)$. In Figure 1, the total angle of the wedge is defined by $\Omega = \alpha\pi$ and $\alpha = \frac{2m}{m+1}$ is the wedge angle parameter. The velocity $u = U(x,t)$ is considered at the outer edge of the boundary layer, and then outside of the boundary layer:

$$-\frac{1}{\rho}\frac{\partial p}{\partial x} = \frac{\partial U}{\partial t} + U\frac{\partial U}{\partial x}$$

which gives that,

$$-\frac{1}{\rho}\frac{\partial p}{\partial x} = \frac{\upsilon^2}{\delta^{2m+2}}\left[m - \tilde{C}(m+1)\right]x^{2m-1}$$

where $\tilde{C} = \frac{\delta^m}{\upsilon x^{m-1}}\frac{\partial \delta}{\partial t}$ is taken to be a constant and thus it can be treated as a dimensionless measure of the unsteadiness parameter. The physical configuration of the model is shown in Figure 1.

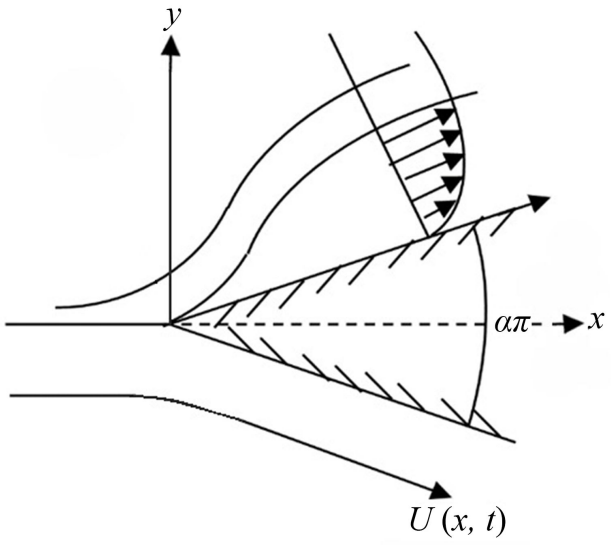

Figure 1. Physical configuration of the model.

The equations relevant to the unsteady two-dimensional problem are governed by the following system of non-linear partial differential equations under the competent boundary layer approximation are given as follows:

Continuity equation:

$$\frac{\partial u}{\partial x} + \frac{\partial v}{\partial y} = 0 \tag{1}$$

$$\frac{\partial u_p}{\partial x} + \frac{\partial v_p}{\partial y} = 0 \tag{2}$$

Momentum equation:

$$\frac{\partial u}{\partial t} + u\frac{\partial u}{\partial x} + v\frac{\partial u}{\partial y} = \upsilon\frac{\partial^2 u}{\partial y^2} - \frac{1}{\rho}KN\left(u - u_p\right) + \frac{\upsilon^2}{\delta^{2m+2}}\left[m - \tilde{C}(m+1)\right]x^{2m-1} \tag{3}$$

$$m_p\left(\frac{\partial u_p}{\partial t}+u_p\frac{\partial u_p}{\partial x}+v_p\frac{\partial u_p}{\partial y}\right)=KN\left(u-u_p\right) \tag{4}$$

It provides the boundary condition for the horizontal wedges as follows:

$$\left.\begin{aligned} u=u_p=0 \text{ at } y=0 \\ u=u_p=U\left(x,t\right) \text{ at } y\to\infty \end{aligned}\right\} \tag{5}$$

Non-Dimensional Analysis

Steric expressed as a non-dimensionless parameter,

$$x^*=\frac{U}{\upsilon}x,\ y^*=\frac{U}{\upsilon}y,\ u^*=\frac{u}{U},\ v^*=\frac{v}{U},\ u_p^*=\frac{u_p}{U},\ v_p^*=\frac{v_p}{U},\ t^*=\frac{U^2}{\upsilon}t$$

Using the above quantities, Equations (1)-(4) become

$$\frac{\partial u}{\partial x}+\frac{\partial v}{\partial y}=0 \tag{6}$$

$$\frac{\partial u_p}{\partial x}+\frac{\partial v_p}{\partial y}=0 \tag{7}$$

$$\frac{\partial u}{\partial t}+u\frac{\partial u}{\partial x}+v\frac{\partial u}{\partial y}=\frac{\partial^2 u}{\partial y^2}-R\left(u-u_p\right)+\left(\frac{1}{R_e}\right)^{2m+2}\left[m-\tilde{C}\left(m+1\right)\right]x^{2m-1} \tag{8}$$

$$\frac{\partial u_p}{\partial t}+u_p\frac{\partial u_p}{\partial x}+v_p\frac{\partial u_p}{\partial y}=\frac{1}{G}\left(u-u_p\right) \tag{9}$$

Its corresponding boundary condition for the horizontal wedges as follows:

$$\left.\begin{aligned} u=u_p=0, v=v_p=0 \text{ at } y=0 \\ u=u_p=1 \text{ at } y\to\infty \end{aligned}\right\} \tag{10}$$

where, $\tilde{C}=\frac{\delta^m}{\upsilon x^{m-1}}\frac{\partial\delta}{\partial t}$ is a constant, this treated as a dimensionless measure of the unsteadiness parameter.

$R=\frac{\upsilon KN}{\rho U^2}$ is the Fluid Concentration Parameter, the value of R physically represents the ratio of fluid density to the total mixture density, indicating the relative dominance of the fluid phase in a dusty fluid flow.

$R_e=\frac{\delta U}{\upsilon}$ is the Reynolds number.

$m=\frac{\alpha}{2-\alpha}$ is a dimensionless quantity, which is the power of the length co-ordinate x of the velocity of the potential flow.

α is the dimensionless wedge angle parameter.

$G=\frac{m_p U^2}{\upsilon KN}$ is the particle mass parameter.

3. Solution Procedure

The solution procedure is the systematic approach employed to solve a problem or address a challenge. The solution procedure serves as a systematic framework

that guides the computation from the initial formulation to the final solution. From the concept of the above discussion, for explicit finite difference method has been used to solve Equations (6)-(9) subject to the boundary conditions given by (10). A trial-and-error approach has been used to determine suitable step sizes and relaxation parameters in order to ensure numerical stability and convergence of the explicit finite difference solution. To obtain the difference equations, the region of the flow is divided into a grid or mesh of lines parallel to x and y axes where x axis is along the plate and y -axis is normal to the plate. Here, we consider that the plate of length $x_{\max}$ *i.e.* x varies from 0 to 40 and regard $y_{\max}$ as corresponding to $y \to \infty$ *i.e.* y varies from 0 to 8. The grid pair has been taken (m, n) = (100, 80).

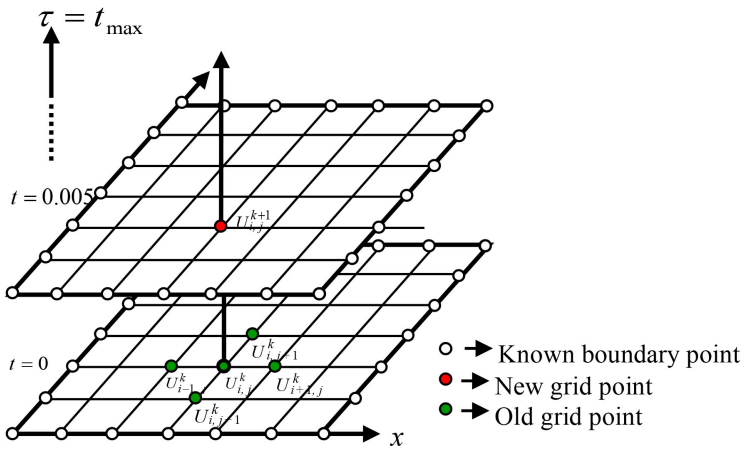

It is assumed that Δy is a constant mesh size along y direction and taken as follows, $\Delta x = 0.5$, $\Delta y = 0.1333$ with the smaller time-step, $\Delta \tau = 0.005$. Let U and W denote the values of u and w at the end of a time step, respectively. There are used explicit finite difference approximations on the Equations (6)-(10).

Specifically the forward finite difference approximation has been used for the terms $\frac{\partial u}{\partial t}, \frac{\partial u_p}{\partial t}, \frac{\partial u}{\partial x}$ and $\frac{\partial u_p}{\partial x}$; whereas the backward finite difference approximation has been used for the terms $\frac{\partial u}{\partial y}, \frac{\partial v}{\partial y}, \frac{\partial u_p}{\partial y}$ and $\frac{\partial v_p}{\partial y}$, and the central finite difference approximation has been used for the terms $\frac{\partial^2 u}{\partial y^2}$ and $\frac{\partial^2 u_p}{\partial y^2}$ to get the suitable evaluation in the solution domain. Finally, the finite difference forms of the given equations have been found which are as follows:

For Fluid phase:

$$V_{i,j}^k = V_{i,j-1}^k - \frac{l}{h}\left(U_{i+1,j}^k - U_{i,j}^k\right)$$

$$U_{i,j}^{k+1} = U_{i,j}^k + \frac{\tau}{l^2}\left(U_{i,j+1}^k - 2U_{i,j}^k + U_{i,j-1}^k\right) - \frac{\tau}{h}U_{i,j}^k\left(U_{i+1,j}^k - U_{i,j}^k\right)$$

$$-\frac{\tau}{l}V_{i,j}^{k}\left(U_{i,j}^{k}-U_{i,j-1}^{k}\right)-\tau R\left(U_{i,j}^{k}-Up_{i,j}^{k}\right)+\left(\frac{1}{R_e}\right)^{2m+2}\left[m-\tilde{C}\left(m+1\right)\right]\tau X_{i,j}^{2m-1}$$

For Dust Fluid phase:

$$Vp_{i,j}^{k}=Vp_{i,j-1}^{k}-\frac{l}{h}\left(Up_{i+1,j}^{k}-Up_{i,j}^{k}\right)$$

$$Up_{i,j}^{k+1}=Up_{i,j}^{k}+\frac{\tau}{G}\left(U_{i,j}^{k}-Up_{i,j}^{k}\right)-\frac{\tau}{h}Up_{i,j}^{k}\left(Up_{i+1,j}^{k}-Up_{i,j}^{k}\right)-\frac{\tau}{l}V_{i,j}^{k}\left(Up_{i,j}^{k}-Up_{i,j-1}^{k}\right)$$

The subscripts i and j designate the grid points with x and y co-ordinates respectively and the superscript prepresents a value of time, $t=p\Delta\tau$ where $p=0,1,2,3,\cdots$ from the initial condition.

4. Results and Discussion

In this research, the governing equations are organized using standard transformation technology. The explicit finite difference method is used in the transformed governing equations. The MATLAB programming language is utilized to construct appropriate software for resolving these equations. The governing equations are then numerically solved. The necessary values for velocity and concentration profile in various grapes are displayed with varying values of relevant parameters.

Effects of Various Parameters

To investigate the physical properties of the problem, the numerical values of different relevant parameters namely wedge angle (α), particle mass parameter (G), fluid concentration parameter (R), Reynolds number (R_e) are represented graphically through Figures 2-13.

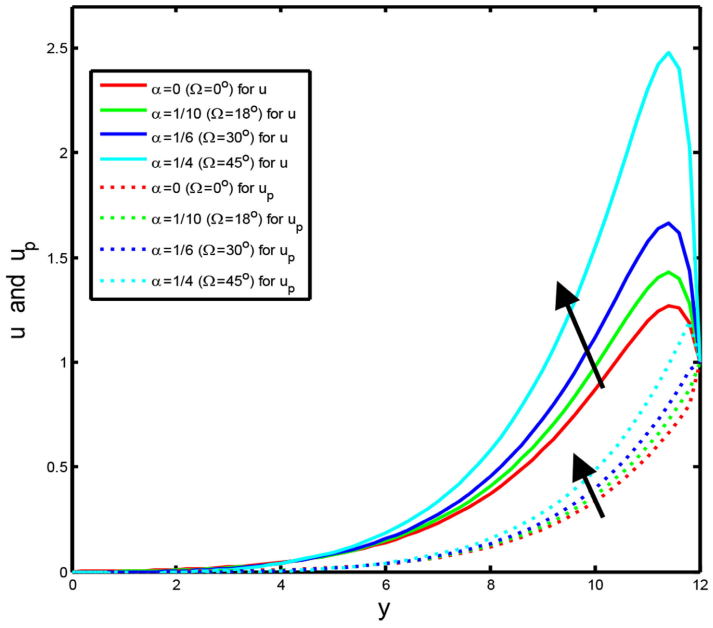

Figure 2. Effects of the wedges angle α on the velocity u and u_p for fixed values of $G=20$, $\tilde{C}=1$, $R=0.2$, $R_e=2$.

Figures 2-5 depict the effect of wedge angle (α), particle mass parameter (G), Fluid concentration number (R), and the Reynolds number (R_e) on the clean fluid velocity (u) and dust particle velocity (u_p). Figure 2 shows that velocity increases with the increase in wedge angle (α). Figures 3-5 depict that velocity decreases with the increase in particle mass parameter (G), Fluid concentration number (R), and the Reynolds number (R_e).

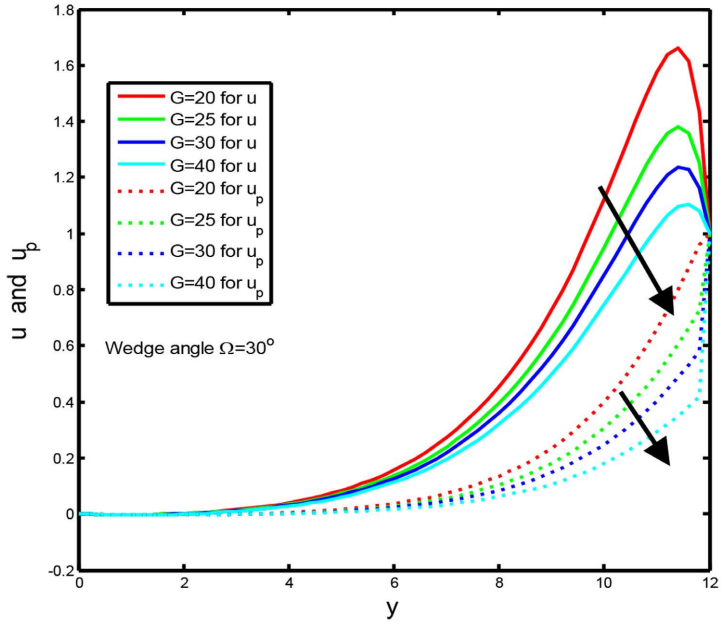

Figure 3. Effects of the particle mass parameter G on the velocity u and u_p for fixed values of $\tilde{C}=1$, $R=0.2$, $R_e=2$, $\alpha=1/6$.

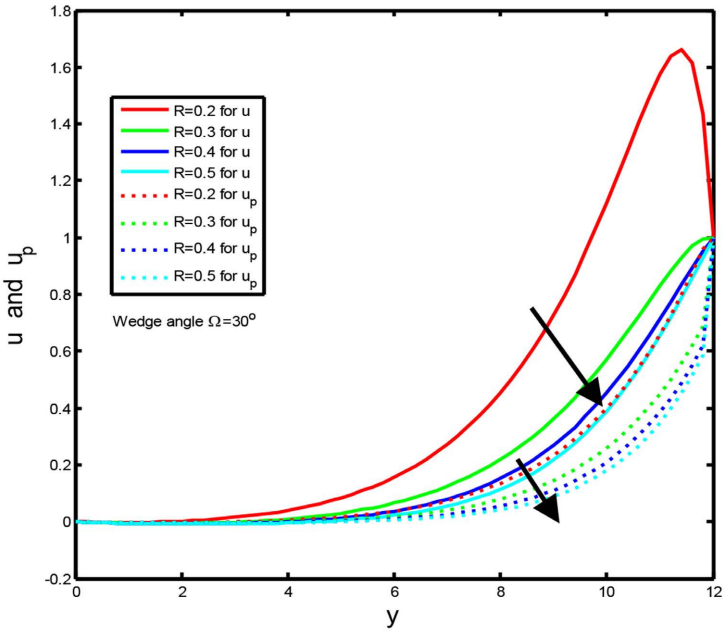

Figure 4. Effects of the Fluid concentration number R on the velocity u and u_p for fixed values of $G=20$, $\tilde{C}=1$, $R_e=2$, $\alpha=1/6$.

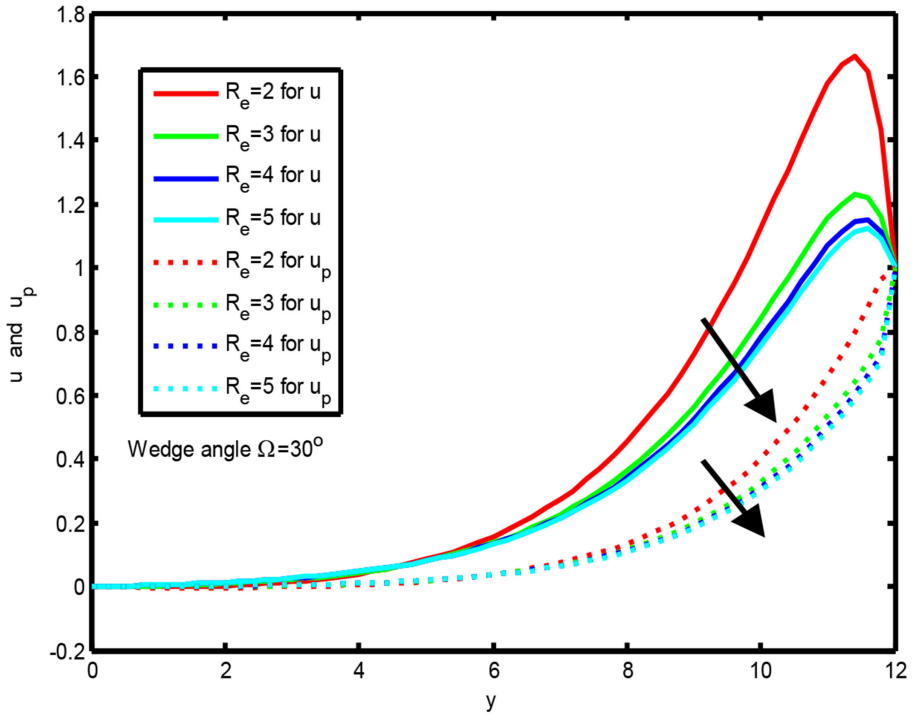

Figure 5. Effects of the Reynolds number R_e on the velocity u and u_p for fixed values of $G = 20$, $\tilde{C} = 1$, $R = 0.2$, $\alpha = 1/6$.

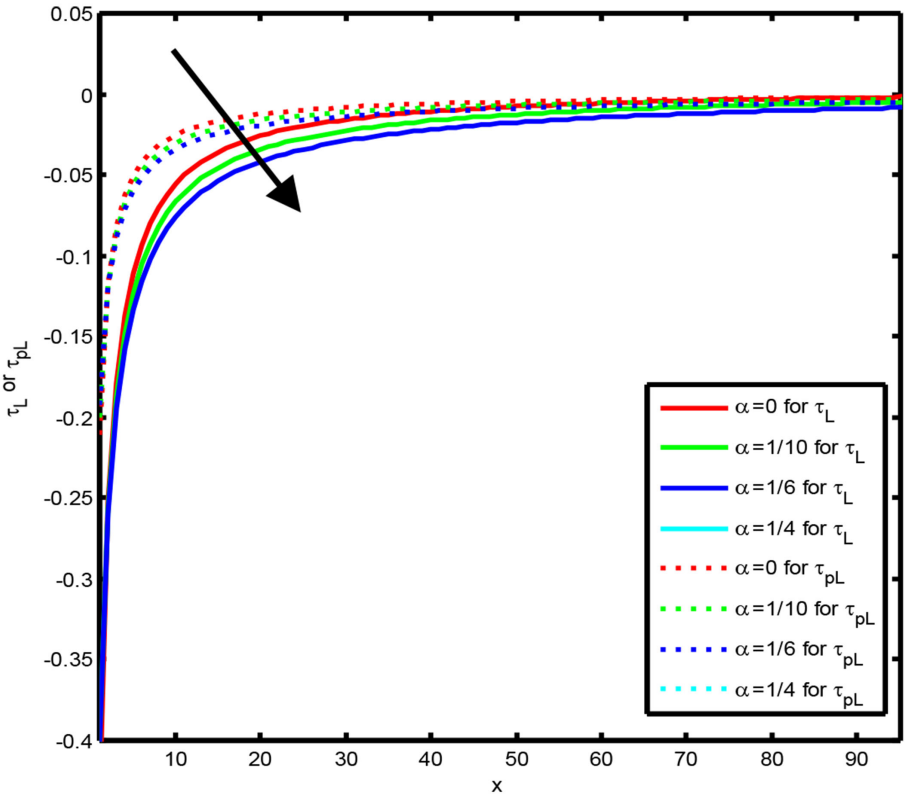

Figure 6. Effects of the wedges angle α on the local shear stress for fixed values of $G = 20$, $\tilde{C} = 1$, $R = 0.2$, $R_e = 2$.

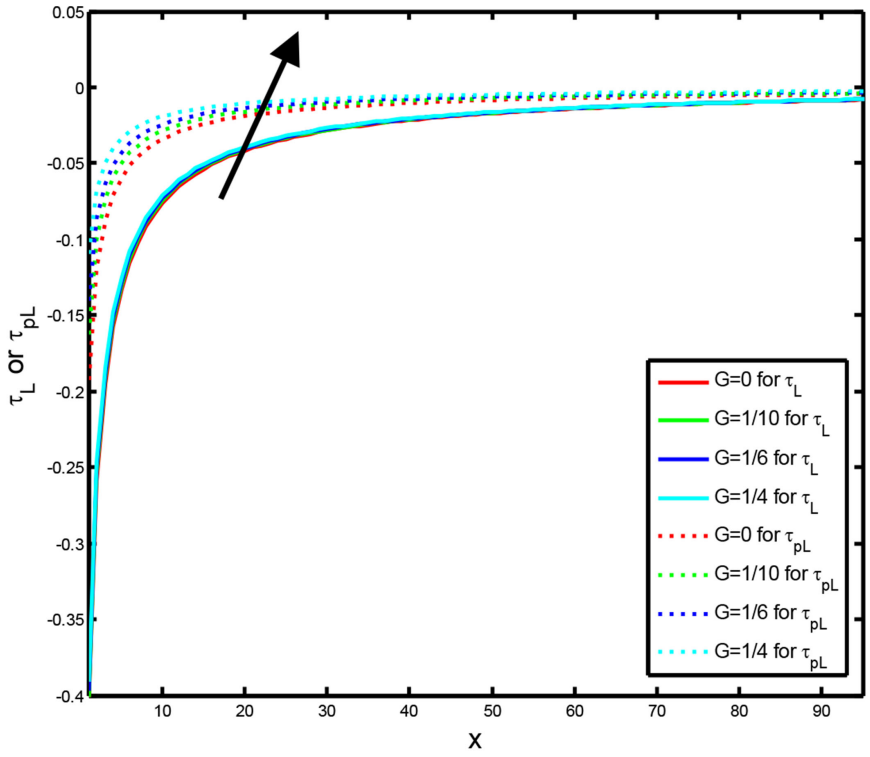

Figure 7. Effects of the particle mass parameter G on the local shear stress for fixed values of $\tilde{C}=1$, $R=0.2$, $R_e=2$, $\alpha=1/6$.

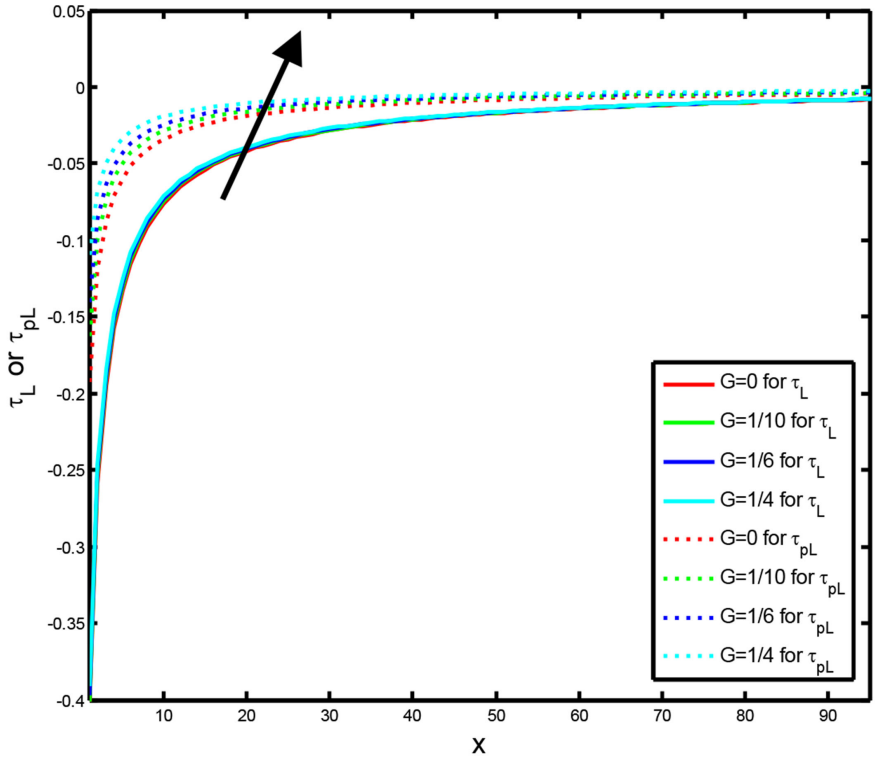

Figure 8. Effects of the Fluid concentration number R on the local shear stress for fixed values of $G=20$, $\tilde{C}=1$, $R_e=2$, $\alpha=1/6$.

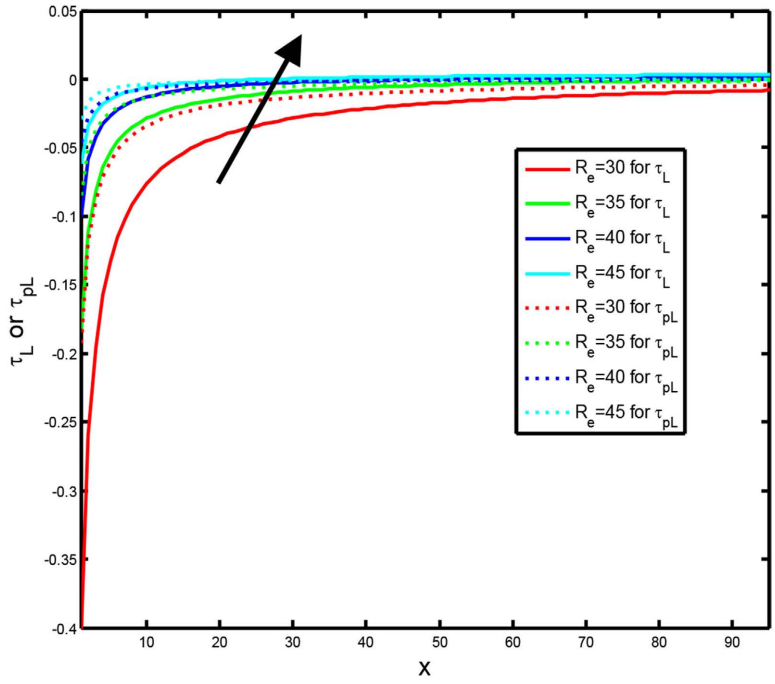

Figure 9. Effects of the Reynolds number R_e on the local shear stress for fixed values of $G = 20$, $\tilde{C} = 1$, $R = 0.2$, $\alpha = 1/6$.

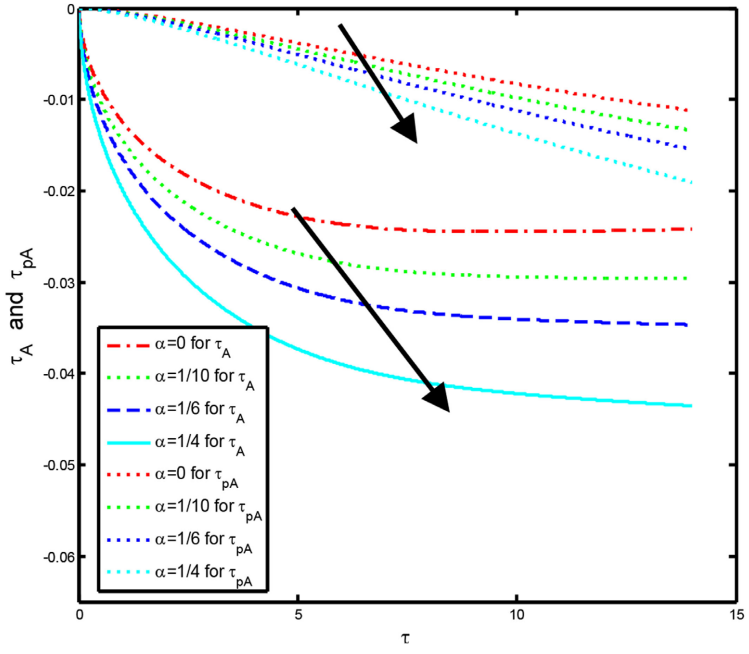

Figure 10. Effects of the wedge angle α on the average shear stress for fixed values of $G = 20$, $\tilde{C} = 1$, $R = 0.2$, $R_e = 2$.

For an increasing particle mass parameter (G), the decline in fluid and dust-phase velocities is due to the increased inertia of the dust particles. Heavier particles resist acceleration, exert a larger drag force on the fluid, causing momentum transfer, loss of fluid kinetic energy, and a reduction in both velocities.

The effect of wedge angle (α), particle mass parameter (G), Fluid concentration number (R), the Reynolds number (R_e) for clear and dusty fluid, and the local shear stress (τ_L) and (τ_{pL}), show in Figures 6-9. Figure 6 shows that local shear stress decreases with the increase in wedge angle (α). From Figures 7-9, it represents that local shear stress increases with the increase in particle mass parameter (G), Fluid concentration number (R), and the Reynolds number (R_e).

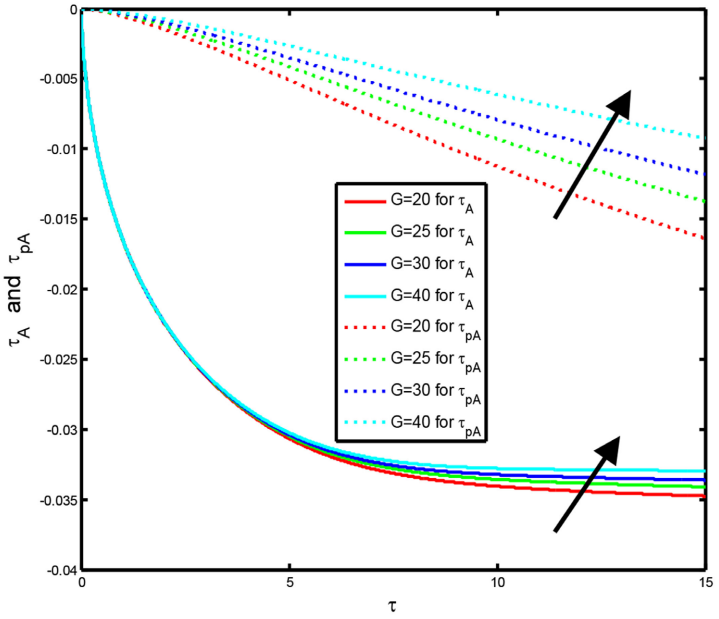

Figure 11. Effects of the particle mass parameter G on the average shear stress for fixed values of $\tilde{C}=1$, $R=0.2$, $R_e=2$, $\alpha=1/6$.

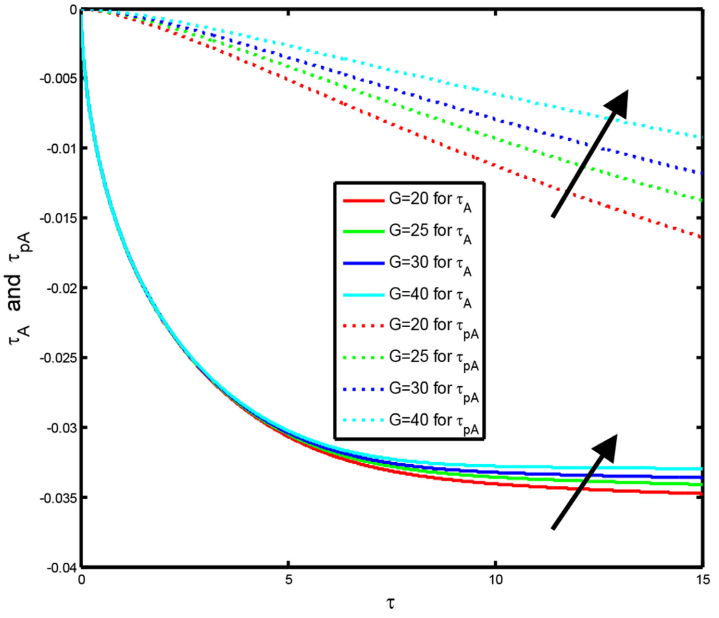

Figure 12. Effects of the Fluid concentration number R on the average shear stress for fixed values of $G=20$, $\tilde{C}=1$, $R_e=2$, $\alpha=1/6$.

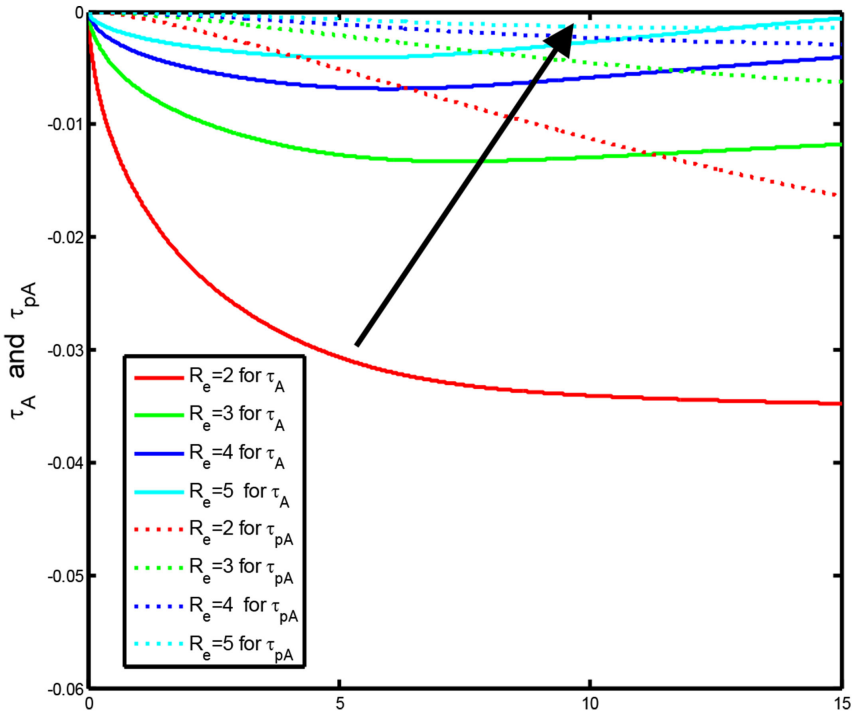

Figure 13. Effects of the Reynolds number R_e on the average shear stress for fixed values of $G = 20$, $\tilde{C} = 1$, $R_e = 2$, $\alpha = 1/6$.

The effect of wedge angle (α), particle mass parameter (G), Fluid concentration number (R), the Reynolds number (R_e) for clear and dusty fluid, and the average shear stress for velocity (τ_A) and (τ_{pA}) are shown in **Figures 10-13**. **Figure 10** displays that average shear stress decreases with the increase in wedge angle (α). From **Figures 11-13**, it marks that the average shear stress increases with the increase in particle mass parameter (G), Fluid concentration number (R), and the Reynolds number (R_e).

5. Conclusions

The physical properties are graphically discussed for four different values of parameters, namely Wedge angle (α), particle mass parameter (G), fluid concentration parameter (R)and Reynolds number (R_e). Based on the graphical representation of results and discussion, some important findings are mentioned as follows:

1) The velocity for clear fluid and dust phase increases with the increase of wedge angle α, while it decreases with the increase of G, R, R_e.

2) The local shear stress for clear fluid and dust phase decreases with the increase of wedge angle α, while it increases with the increase of G, R, R_e.

3) The average shear stress for clear fluid and dust phase decreases with the increase of wedge angle α, while it increases with the increase of G, R, R_e.

Conflicts of Interest

The authors declare no conflicts of interest regarding the publication of this paper.

References

[1] Falkner, V.M. and Skan, S.W. (1931) Some Approximate Solutions of the Boundary Layer Equations. *Philosophical Magazine*, **12**, 865-896.

[2] Rajagopal, K.R., Gupta, A.S. and Na, T.Y. (1983) A Note on the Falkner-Skan Flows of a Non-Newtonian Fluid. *International Journal of Non-Linear Mechanics*, **18**, 313-320. https://doi.org/10.1016/0020-7462(83)90028-8

[3] Datta, N., Dalal, D.C. and Mishra, S.K. (1993) Unsteady Heat Transfer to Pulsatile Flow of a Dusty Viscous Incompressible Fluid in a Channel. *International Journal of Heat and Mass Transfer*, **36**, 1783-1788. https://doi.org/10.1016/s0017-9310(05)80164-4

[4] Kumari, M. and Gorla, R.S.R. (1997) Combined Convection along a Non-Isothermal Wedge in a Porous Medium. *Heat and Mass Transfer*, **32**, 393-398. https://doi.org/10.1007/s002310050136

[5] Hossain, M.A., Munir, M.S., Hafiz, M.Z. and Takhar, H.S. (2000) Flow of a Viscous Incompressible Fluid of Temperature Dependent Viscosity Past a Permeable Wedge with Uniform Surface Heat Flux. *Heat and Mass Transfer*, **36**, 333-341. https://doi.org/10.1007/s002310000079

[6] Anwar Hossain, M., Bhowmick, S. and Gorla, R.S.R. (2006) Unsteady Mixed-Convection Boundary Layer Flow along a Symmetric Wedge with Variable Surface Temperature. *International Journal of Engineering Science*, **44**, 607-620. https://doi.org/10.1016/j.ijengsci.2006.04.007

[7] Attia, H.A. (2006) Unsteady MHD Couette Flow and Heat Transfer of Dusty Fluid with Variable Physical Properties. *Applied Mathematics and Computation*, **177**, 308-318. https://doi.org/10.1016/j.amc.2005.11.010

[8] Rajput, S., Verma, A.K., Bhattacharyya, K. and Chamkha, A.J. (2021) Unsteady Nonlinear Mixed Convective Flow of Nanofluid over a Wedge: Buongiorno Model. *Waves in Random and Complex Media*, **34**, 4059-4073. https://doi.org/10.1080/17455030.2021.1987586

[9] Watanabe, T. (1991) Forced and Free Mixed Convection Boundary Layer Flow with Uniform Suction or Injection on a Vertical Flat Plate. *Acta Mechanica*, **89**, 123-132. https://doi.org/10.1007/bf01171250

[10] Ishak, A., Nazar, R. and Pop, I. (2007) Falkner-Skan Equation for Flow Past a Moving Wedge with Suction or Injection. *Journal of Applied Mathematics and Computing*, **25**, 67-83. https://doi.org/10.1007/bf02832339

[11] Mahanthesh, B., Animasaun, I.L., Rahimi-Gorji, M. and Alarifi, I.M. (2019) Quadratic Convective Transport of Dusty Casson and Dusty Carreau Fluids Past a Stretched Surface with Nonlinear Thermal Radiation, Convective Condition and Non-Uniform Heat Source/Sink. *Physica A*: *Statistical Mechanics and Its Applications*, **535**, Article 122471. https://doi.org/10.1016/j.physa.2019.122471

[12] Abbas, W., Mekheimer, K.S., Ghazy, M.M. and Moawad, A.M.A. (2020) Thermal Radiation Effects on Oscillatory Squeeze Flow with a Particle-Fluid Suspension. *Heat Transfer*, **50**, 2129-2149. https://doi.org/10.1002/htj.21971

[13] Chandrawat, R.K., Joshi, V. and Kanchan, S. (2022) Numerical Simulation of Interface Tracking between Two Immiscible Micropolar and Dusty Fluids. *Materials Today*: *Proceedings*, **50**, 1199-1209. https://doi.org/10.1016/j.matpr.2021.08.069

[14] Saxena, P. and Agarwal, M. (2014) Unsteady Flow of a Dusty Fluid between Two Parallel Plates Bounded above by Porous Medium. *International Journal of Engineering, Science and Technology*, **6**, 27-33. https://doi.org/10.4314/ijest.v6i1.3

[15] Islam, M.R. and Nasrin, S. (2021) Unsteady Couette Flow of Dusty Fluid Past Between Two Riga Plates. *European Journal of Scientific Research*, **159**, 18-32.

[16] Attia, H.A. and Ewis, K.M. (2019) Magnetohydrodynamic Flow of Continuous Dusty Particles and Non-Newtonian Darcy Fluids between Parallel Plates. *Advances in Mechanical Engineering*, **11**, 1-11. https://doi.org/10.1177/1687814019857349

[17] Attia, H.A., Aboul-Hassan, A.L., Abdeen, M.A.M. and Abdin, A.E.D. (2014) MHD Flow of a Dusty Fluid between Two Infinite Parallel Plates with Temperature Dependent Physical Properties under Exponentially Decaying Pressure Gradient. *Bulgarian Chemical Communications*, **46**, 320-329.

[18] Attia, H.A. (2005) Unsteady Flow of a Dusty Conducting Fluid between Parallel Porous Plates with Temperature Dependent Viscosity. *Turkish Journal of Physics*, **29**, 257-267.

[19] Abbas, W., Khaled, O., Beshir, S., Abdeen, M. and Elshabrawy, M. (2023) Analysis of Chemical, Ion Slip, and Thermal Radiation Effects on an Unsteady Magnetohydrodynamic Dusty Fluid Flow with Heat and Mass Transfer through a Porous Media between Parallel Plates. *Bulletin of the National Research Centre*, **47**, Article No. 49. https://doi.org/10.1186/s42269-023-01024-x